Scattering Properties of One-Dimensional Aperiodically-Ordered Strip Arrays Based on Two-Symbol Substitutional Sequences

Vincenzo Galdi, *Senior Member, IEEE*, Giuseppe Castaldi, Vincenzo Pierro, Innocenzo M. Pinto, *Senior Member, IEEE*, and Leopold B. Felsen, *Life Fellow, IEEE*

This paper is dedicated to the memory of Prof. Leo Felsen, mentor and friend. Prof. Felsen supervised this research project and contributed to the initial editing of the manuscript, but did not see the final version.

***Abstract*—This paper is concerned with a study of the two-dimensional (2-D) time-harmonic scattering by aperiodically-ordered 1-D planar strip arrays based on two-symbol substitutional sequences, under Kirchhoff physical-optics approximation. In this connection, theoretical results from solid-state physics, dwelling on concepts from discrete geometry and number theory, are briefly reviewed and applied to the characterization of the scattering signatures of the above physical configuration. Parametric studies are presented in order to flesh out some of the above concepts and to highlight wave-features which are thought as being representative of a fairly broad class of regular non-periodic scatterers. Potential applications are also envisaged.**

***Index Terms*—Aperiodic order, quasicrystals, scattering, substitutional sequences.**

I. Introduction

THE pioneering studies, during the 1960s and 1970s, of *aperiodic tilings* exhibiting *long-range* order (see [1]–[3] for an introductory review), and the first experimental evidence, linked with the discovery of "quasicrystals" in the 1980s [4], [5], have motivated a growing interest in the study of *aperiodically-ordered* geometries in the largely unexplored "gray zone" that separates *perfect periodicity* from *absolute randomness*.

Within this context, the possibility of unveiling new phenomena and envisaging new applications in electromagnetics (EM) engineering has stimulated the investigation of the electrodynamic observables induced by aperiodically-ordered geometries, with main focus on photonic bandgap (PBG) quasicrystals (see [6]–[19] for a sparse sampling). Against this background, in an ongoing series of investigations [20]–[22], we have concentrated on the time-harmonic radiation properties of representative classes of one-dimensional (1-D) and 2-D aperiodic configurations, also addressing potential engineering applications to thinned and/or multibeam (possibly reconfigurable) antenna arrays. In all of these examples, either the element excitations [20], [21] or the inter-element spacings [22] were somehow *constrained*.

In the present study, we move one step further by studying the time-harmonic oblique-plane-wave-excited scattering signatures of a *fairly broad*, though relatively simple, class of 1-D aperiodically-ordered arrays, composed of two arbitrary types of strips and two arbitrary inter-element spacings, arranged according to a *two-symbol substitutional sequence*. Capitalizing on a number of theoretical results from discrete geometry and solid-state physics [23]–[29], we address the analytic parameterization of the arising scattering signatures in terms of the well-known Floquet/Bragg-type spectral constituents that are typically encountered in the study of *strictly* or *weakly-perturbed periodic* structures (see, e.g., [30]–[34]), plus other constituents that have no counterpart in periodic structures. Moreover, we present a series of parametric studies, in order to flesh out the above concepts and to highlight the role of the various parameters and degrees of freedom.

Accordingly, the remainder of the paper is laid out as follows. Section II introduces the problem geometry and formulation, based on a Kirchhoff physical-optics (PO) model. Section III briefly reviews the theoretical results borrowed from solid-state physics for the characterization of the scattering signatures of the aperiodically-ordered arrays of interest; the interested reader may address the cited references [23]–[29] for a full formal account. Section IV illustrates the numerical studies carried out for representative aperiodic geometries (Fibonacci, Thue-Morse, period-doubling, Rudin-Shapiro) and various parameter configurations (scale-ratio, strip width and constitutive properties, array size). Section V contains some concluding remarks.

II. Problem Geometry and Formulation

A 1-D array of coplanar strips centered at $x = x_n$, $n = 0, 1, \ldots, N-1$, and assumed to be infinitely long in the y-direction, is illuminated by a time-harmonic [$\exp(j\omega t)$ time dependence], unit-amplitude, plane-wave with y-polarized electric field $E^i(x,z) = \exp[-jk_0(x\sin\theta^i - z\cos\theta^i)]$, where

Manuscript received March 15, 2006; revised October 11, 2006.

V. Galdi is with the Waves Group, Department of Engineering, University of Sannio, I-82100 Benevento, Italy (e-mail: vgaldi@unisannio.it).

G. Castaldi is with the Waves Group, Department of Engineering, University of Sannio, I-82100 Benevento, Italy (e-mail: castaldi@unisannio.it).

V. Pierro is with the Waves Group, Department of Engineering, University of Sannio, I-82100 Benevento, Italy (e-mail: pierro@unisannio.it).

I. M. Pinto is with the Waves Group, Department of Engineering, University of Sannio, I-82100 Benevento, Italy (e-mail: pinto@sa.infn.it).

L. B. Felsen, *(deceased)*, was with the Department of Aerospace and Mechanical Engineering and the Department of Electrical and Computer Engineering, Boston University, Boston, MA 02215 USA, and also with Polytechnic University, Brooklyn, NY 11201 USA.

Digital Object Identifier 10.1109/TAP.2007.897228

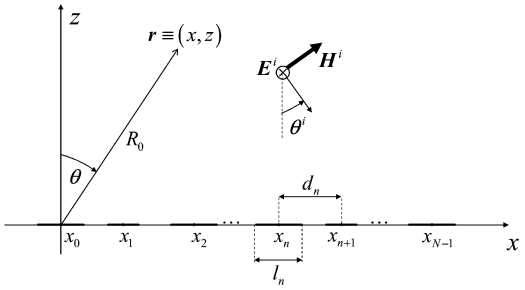

Fig. 1. Problem geometry. A time-harmonic plane wave with y-polarized electric field illuminates a 1-D aperiodic array of N coplanar strips placed along the x-axis. The strip centers, widths, center-to-center inter-element distance, and reflection coefficients are denoted by x_n, l_n, d_n, and Γ_n, respectively ($n = 0, \ldots, N-1$). Also shown is the 2-D polar (R_0, θ) reference system centered at $x_0 = 0$.

$k_0 = \omega\sqrt{\epsilon_0\mu_0} = 2\pi/\lambda_0$ denotes the free-space wavenumber (with λ_0 = free-space wavelength), and θ^i denotes the incidence angle relative to the z-axis (see Fig. 1). The strip with center location x_n has width l_n, and spectral reflection coefficient Γ_n, $n = 0, 1, \ldots, N-1$. Also shown in Fig. 1 is the 2-D polar $[R_0 \equiv \sqrt{x^2+z^2}, \theta \equiv \arctan(z/x)]$ reference system centered at the array end-point $x_0 = 0$. Using a standard Kirchhoff PO approximation (E-formulation, neglecting the inter-element coupling) [35] for the y-directed scattered far field in the Fraunhofer region ($R_0 \gg 2x_{N-1}^2/\lambda_0$), and introducing the spectral variables $k_x = k_0 \sin\theta, k_x^i = k_0 \sin\theta^i, k_z = \sqrt{k_0^2 - k_x^2} = k_0 \cos\theta$, one obtains the following approximate spectral model

$$E_N^s(k_x, k_x^i) \sim \sum_{n=0}^{N-1} F_n(k_x, k_x^i) \exp\left[j\left(k_x - k_x^i\right) x_n\right] \quad (1)$$

where the single-element scattering response (SESR)

$$F_n(k_x, k_x^i) = \Gamma_n(k_x^i) k_z \sqrt{\frac{2}{\pi k_0 R_0}} \frac{\sin\left[\frac{\left(k_x - k_x^i\right) l_n}{2}\right]}{k_x - k_x^i} \times \exp\left[-j\left(k_0 R_0 - \frac{\pi}{4}\right)\right] \quad (2)$$

can be controlled, in principle, by varying the strip width l_n and/or its reflection coefficient Γ_n. It is assumed that the strip widths l_n, the inter-element spacings $d_n \equiv x_{n+1} - x_n$, and the spectral reflection coefficients Γ_n [and hence the SESR F_n in (2)] can take on only two possible values (labeled with subscripts "$_a$" and "$_b$", respectively) chosen according to a symbolic sequence generated from a two-symbol alphabet

$$\Psi_N = s_0 s_1 \cdots s_{N-1}, \quad s_n \in \{a, b\}. \quad (3)$$

Attention is focused on a particular arrangement within rather general aperiodically-ordered array configurations based on *substitutional sequences* [28], [29] generated by substitution rules of the type

$$\begin{cases} \xi(a) = \alpha_{pq}(a, b) \\ \xi(b) = \beta_{rs}(a, b) \end{cases} \quad (4)$$

where $\psi_{uv}(\psi \equiv \alpha, \beta)$ denotes a sequence of total length $u + v$ consisting of some permutation of a number u of "a" symbols and a number v of "b" symbols. Starting from a given initial string ("seed"), a substitutional sequence is generated by iterating the substitution rules in (4) *ad infinitum*.

III. Summary of Relevant Theoretical Results

A. Generalities

Our present investigation is structured according to *primitive* substitution rules, characterized by $(p + s)qr \neq 0$, which generate infinite, generally-aperiodic sequences [28], [29]. For these geometries, exploiting some theoretical results available in the discrete-geometry and crystallography literature [23]–[29], analytic parameterization of typical aperiodic-order-induced wave-dynamical phenomenologies can be addressed in terms of Bragg-type spectral constituents that are also encountered in the study of *periodic* structures, plus certain *diffused* "singular-continuous" and "absolutely-continuous" constituents that have no periodic counterpart (see, e.g., [25], [26] for details). As well known, Bragg-type spectral constituents are associated with field intensities which scale as $\sim N^2$ (N being the size of the array), yielding Dirac-delta spectral peaks in the infinite-array limit. Loosely speaking, singular-continuous spectral constituents are associated with field-intensity scaling of the type $\sim N^\alpha, 1 < \alpha < 2$, yielding *weaker* (i.e., non-Dirac-delta) spectral peaks; they are typically associated with intermediate forms of aperiodic order, and generally exhibit *multifractal* character [25], [26]. Conversely, absolutely-continuous constituents are associated with field-intensity scaling of the type $\sim N$, yielding *noise-like flat* background spectra; such behavior is typical of random or quasirandom geometries.

Within this framework, a key role is played by the *substitution matrix*

$$\underline{\underline{S}} = \begin{bmatrix} p & q \\ r & s \end{bmatrix} \quad (5)$$

which describes the symbol distribution in (4), [2], [28], [29]. It can be shown that, for the case of primitive substitution rules, the substitution matrix in (5) admits two *real* eigenvalues Λ_1 and Λ_2, with $\Lambda_1 > |\Lambda_2|$ [28], [29]. Moreover, in the infinite-sequence limit, the two symbols occur with *well-defined* frequencies, with the symbol-frequency ratio (SFR), i.e., the ratio between the numbers of "a" and "b" symbols, approaching the value [28], [29]

$$\chi = \lim_{N\to\infty} \frac{N_a}{N_b} = \frac{\Lambda_1 - s}{q} = \frac{r}{\Lambda_1 - p}, N_a + N_b = N. \quad (6)$$

For these geometries, a comprehensive characterization of the Bragg-type mode (BM) spectra has been addressed in [28], [29], following up on the pioneering analysis by Bombieri and Taylor [23], [24] based on the so-called Pisot-Vijayaraghavan (PV) condition. The analysis in [28], [29] is based on a working model that, in spite of the slightly different notation, is equivalent to the PO spectral model in (1). This model is first recast in

suitable recursive forms, and the analysis is eventually reduced to the study of the fixed-points (mod 2π) of the 2-D map

$$\underline{\Phi}_{M+1} = \underline{\underline{\mathcal{S}}}^{M} \cdot \underline{\Phi}_0, \underline{\Phi}_0 = \begin{bmatrix} \left(k_x - k_x^i\right) d_a \\ \left(k_x - k_x^i\right) d_b \end{bmatrix}. \tag{7}$$

The main results, asymptotically valid in the infinite-array limit, can be summarized as follows (see [28], [29] for more details). BM wavenumbers for aperiodic structures, unlike those for the periodic case, are generally *unevenly* spaced. The BM spectrum generally depends on the eigenvalues of the substitution matrix in (5), and on the scale-ratio d_a/d_b. Interestingly, the substitution matrix depends *only on the number of symbols* in the substitution rules, and *not on their ordering*. For *rational* values of the scale-ratio, there exist also "trivial" BM whose wavenumbers *do not* depend on the substitution rules. The modal amplitudes generally do depend on the symbol ordering in the substitution rule for the "nontrivial" BM, as well as on the incident field and the scattering response of the strip elements. Thus, some BM may not be excited for certain particular geometry and/or parameter configurations.

In what follows, the most relevant results are compactly reviewed via the illustration of representative examples, which are strictly related to the parametric studies in Section IV.

B. Examples

1) Trivial BM: These BM can be exhibited by *any* 1-D strip array arrangement (even *random* [36]), *regardless* of the substitution rule. For this reason, such BM are referred to as "trivial". It can be shown that, for *irrational* d_a/d_b, the only trivial BM is $k_x = k_x^i$ (specular reflection), whereas, for *rational* d_a/d_b, there are infinitely many trivial BM at wavenumbers

$$k_{xm} = k_x^i + \frac{2\pi}{d_a} m = k_x^i + \frac{2\pi}{d_b} n, \quad \forall m, n \in \mathbb{Z} : n d_a = m d_b \tag{8}$$

with excitation intensities [28], [29]

$$|E_N^s\left(k_{xm}, k_x^i\right)|^2 \sim N^2 \frac{\left|\chi F_a\left(k_{xm}, k_x^i\right) + F_b\left(k_{xm}, k_x^i\right)\right|^2}{(\chi d_a + d_b)^2}. \tag{9}$$

From (9), it is understood that trivial BM excitation amplitudes depend on the wavenumber only via the SESR F_a and F_b. These modes can be "suppressed", in principle, by properly tuning the array parameter configuration so that

$$F_b\left(k_{xm}, k_x^i\right) = -\chi F_a\left(k_{xm}, k_x^i\right). \tag{10}$$

2) Fibonacci Sequences: Fibonacci sequences are characterized by the following substitution rule, substitution matrix and eigenvalues, and SFR (see [2], [21] for details and alternative generation procedures)

$$\begin{cases} \xi(a) = ab, \\ \xi(b) = a, \end{cases} \underline{\underline{\mathcal{S}}} = \begin{bmatrix} 1 & 1 \\ 1 & 0 \end{bmatrix}, \Lambda_{1,2} = \frac{1 \pm \sqrt{5}}{2}$$
$$\chi = \tau \equiv \frac{1+\sqrt{5}}{2} \quad \text{(Golden Mean)}. \tag{11}$$

It can be shown that the associated nontrivial BM spectrum is given by [28], [29]

$$k_{xmn} = k_x^i + \frac{2\pi(m\tau + n)}{(\tau d_a + d_b)}, m, n \in \mathbb{Z}. \tag{12}$$

This type of spectrum, generated by integer combinations of two *incommensurate* spatial frequencies, is referred to as *quasiperiodic*. It can be shown that no diffused constituents exist, and thus the spectrum is *purely* Bragg-type [2], [26], [29]. The quasiperiodic spectrum in (12) is typical of substitution rules characterized by $|\Lambda_2| < 1$ and $|\Lambda_1 \Lambda_2| = 1$, and represents a particular case of a more general type of spectrum called "infinite-quasiperiodic" [28], [29]. Infinite-quasiperiodic spectra are typical of substitution rules characterized by $|\Lambda_2| < 1$, and are generated by the superposition of an *infinite* number of l-indexed quasiperiodic spectra scaled by a factor $(\Lambda_1 \Lambda_2)^l$; typical examples are provided by generalized-Fibonacci sequences of the type $\xi(a) = a^p b^q, \xi(b) = a$, $2 \le q < p+1$, with s^p denoting the concatenation of p symbols "s" (e.g., $a^3 = aaa$) [28], [29].

3) Thue-Morse Sequences: Thue-Morse (TM) sequences are characterized by the following substitution rule, substitution matrix and eigenvalues, and SFR (see [37] and [38] for details)

$$\begin{cases} \xi(a) = ab, \\ \xi(b) = ba, \end{cases} \underline{\underline{\mathcal{S}}} = \begin{bmatrix} 1 & 1 \\ 1 & 1 \end{bmatrix}, \Lambda_1 = 2, \Lambda_2 = 0, \chi = 1. \tag{13}$$

It can be shown [28], [29] that they admit a *periodic* BM spectrum, identical to that of a periodic structure made of composite "ab" unit cells

$$k_{xm} = k_x^i + \frac{2\pi m}{(d_a + d_b)}, m \in \mathbb{Z}. \tag{14}$$

This should not be surprising, since the two sequences share *the same* substitution matrix. The differences between TM and periodic sequences emerge in the modal excitation amplitudes and the presence of singular-continuous constituents in the TM spectrum. In fact, the spectral signatures of the TM sequence depend critically on the scale-ratio d_a/d_b. For the case $d_a = d_b$, the odd-m amplitudes are zero, and the only surviving (even-m) BM correspond to the trivial ones in (8). Even these BM can be suppressed [cf. (10)] by choosing $F_b = -F_a$, yielding a spectrum *completely devoid* of the BM portion.

As noted previously, TM-based arrays are also characterized by singular-continuous spectral constituents. To the best of our knowledge, the only available results pertain to particular cases where either the inter-element spacings or the SESR are somehow constrained (see, e.g., [26], [39]–[41]). For instance, for the case of equal SESR ($F_a = F_b$) and arbitrary inter-element spacings, it can be shown that there exist singular-continuous modes at wavenumbers [41]

$$k_{\mathrm{xml}} = k_x^i + \frac{2\pi m}{(2l-1)(d_a + d_b)}$$
$$m \in \mathbb{Z}, l \in \mathbb{N}, \mathrm{mod}(m, 2l-1) \neq 0. \tag{15}$$

The above expression also holds for equal inter-element spacings ($d_a = d_b$) and opposite SESR ($F_a = -F_b$) [26], for which the BM spectrum is completely suppressed, thereby rendering

the singular-continuous spectrum most representative. It can be shown that the largest scaling exponent in the field intensity is $\alpha(k_{x12}) = \log 3/\log 2 \approx 1.585$ [41]. Moreover, for a given singular-continuous mode at wavenumber $\bar{k}_x$ and with scaling exponent $\bar{\alpha}$, the same scaling exponent is also found at wavenumbers [41]

$$k_x^{(P,Q)} = k_x^i + 2^{-P}\left[\bar{k}_x - k_x^i + \frac{2\pi Q}{(d_a+d_b)}\right], P, Q \in \mathbb{Z}. \quad (16)$$

The reader is referred to [26], [39]–[41], where the *multifractal* character of the TM singular-continuous spectrum is investigated in detail.

4) Period-Doubling Sequences: Period-doubling (PD) are characterized by the following substitution rule, substitution matrix and eigenvalues, and SFR (see [26], [41] for more details)

$$\begin{cases} \xi(a) = ab, \\ \xi(b) = aa, \end{cases} \underline{\underline{S}} = \begin{bmatrix} 1 & 1 \\ 2 & 0 \end{bmatrix}, \Lambda_1 = 2, \Lambda_2 = -1, \chi = 2. \quad (17)$$

PD-based arrays may exhibit a BM spectrum, whose nature depends critically on the scale-ratio d_a/d_b. In particular, for *irrational* d_a/d_b, only the specular-reflection trivial BM ($k_x = k_x^i$) exists. Conversely, for *rational* $d_a/d_b \neq 1$, one obtains a *periodic-like* BM spectrum [41]

$$k_{xml} = k_x^i + \frac{2\pi m}{2^l d_{av}}, d_{av} = \frac{2d_a + d_b}{3}$$
$$l = 0, 1, \ldots, L, m \in \mathbb{Z}_l \quad (18)$$
$$\mathbb{Z}_l = \left\{ n \in \mathbb{Z} : J_{nl} \equiv \frac{n(d_a - d_b)}{2^l(2d_a + d_b)} \in \mathbb{Z} \right\}$$
$$L = \max\{l \in \mathbb{N} : \mathbb{Z}_l \neq \emptyset\}. \quad (19)$$

For the special case $d_a = d_b$, the BM spectrum assumes the form [28], [29]

$$k_{\mathrm{xml}} = k_x^i + \frac{2\pi m}{2^l d_a}, l \in \mathbb{N}, m \in \mathbb{Z} \quad (20)$$

which is referred to as "infinite-periodic" (superposition of an infinite number of l-indexed periodic spectra scaled by a factor 2^l). PD-based arrays are also characterized by singular-continuous spectral constituents. Also in this case, available results pertain to particular configurations of the inter-element spacings and/or the SESR [26], [41]. For instance, for equal SESR ($F_a = F_b$) and rational scale-ratio d_a/d_b, the singular-continuous modal wavenumbers are still given by (18), but now with [41]

$$l \in \mathbb{N}, m \in \mathbb{Z} : |\cos(J_{ml}\pi)| > 1/\sqrt{2} \quad (21)$$

where J_{ml} is defined in (19). Also in this case the singular-continuous spectrum is characterized by *multifractal* behavior (see [26] and [41] for details).

5) Rudin-Shapiro Sequences: Unlike the previous examples, Rudin-Shapiro (RS) sequences cannot be generated *directly* via two-symbol substitution rules, but rather require a two-step procedure (see [37], [38] for details). One first applies the four-symbol substitution rule, defined on the alphabet $\{a, b, c, d\}$,

$$\xi(a) = ab, \xi(b) = ac, \xi(c) = db, \xi(d) = dc \quad (22)$$

followed by a final projection onto the usual two-symbol alphabet $\{a, b\}$

$$\varphi(a) = a, \varphi(b) = a, \varphi(c) = b, \varphi(d) = b. \quad (23)$$

It can be shown that the SFR is $\chi = 1$ [37], [38], and that the corresponding scattering spectral signatures are characterized by trivial BM only, superposed onto an absolutely-continuous background. If trivial BM are suppressed (e.g., by choosing $d_a = d_b$ and $F_a = -F_b$), the spectrum becomes *purely absolutely-continuous* (no localized peaks).

C. General Substitution Rules

The examples illustrated so far are representative of the BM and diffused spectra encountered in the study of aperiodic arrays based on *general* two-symbol substitution rules. The reader is referred to [28], [29] for a full formal account, as well as a comprehensive classification of the BM spectra. Here, we limit ourselves to emphasizing that the same substitution rule can yield fundamentally different types of BM spectra, depending on the scale-ratio d_a/d_b (see, e.g., the PD sequences in Section III-B.4). In particular, the rational/irrational character of the scale-ratio plays a key role. This raises some important conceptual issues concerning the actual observability of such distinct behaviors in finite-precision computational models or experimental scenarios limited by fabrication tolerances. The reader is referred to [42] (and the references therein) for a theoretical approach. In our investigation, we used an intuitive pragmatic approach to construct *effectively* irrational values of the scale-ratio, based on a *rational* approximation p/q, with $p, q \in \mathbb{N}$ sufficiently large so as to exclude any constructive interference within the spectral range of interest.

IV. Parametric Studies

In this Section, we present a series of numerical simulations in order to flesh out some of the concepts illustrated in Section III, and to understand the role of the various parameters and degrees of freedom. In all simulations, strip widths and inter-element spacings are chosen within the calibrated ranges of validity of the approximate PO model (see, e.g., [33]). The EM observable of interest is the bistatic differential radar cross-section (RCS) (scaled to the free-space wavelength)

$$D_N(\theta) = k_0 R_0 |E_N^s(k_0 \sin\theta^i, k_0 \sin\theta)|^2. \quad (24)$$

Concerning the strip constitutive properties, an idealized model is assumed in which the reflection coefficients $\Gamma_{a,b}$ are independent of the incidence angle; this includes the cases $\Gamma_{a,b} = -1$, $\Gamma_{a,b} = 1$, and $\Gamma_{a,b} = 0$, corresponding to perfectly electric conducting (PEC), perfectly magnetic conducting (PMC), and perfectly transparent strip (lacuna), respectively. No attempt is made at this stage to address physical feasibility issues.

A. Substitution Rules and Scale-Ratio

As a first example, in order to illustrate the role played by the substitution rule, Fig. 2 displays the RCS response for oblique ($\theta^i = 15^o$) plane-wave incidence of several representative aperiodic array configurations, with $N = 100$ identical ($l_a = l_b = 1.2\lambda_0$) PEC ($\Gamma_a = \Gamma_b = -1$) strips, with $d_a = 2.5\lambda_0$

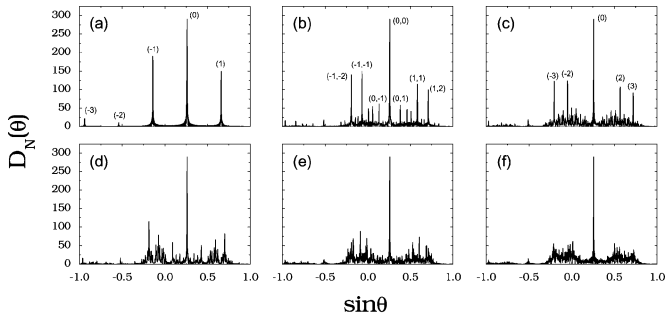

Fig. 2. Geometry as in Fig. 1. RCS responses, for oblique ($\theta^i = 15^o$) plane-wave incidence incidence, of various arrays made of $N = 100$ identical PEC ($\Gamma_a = \Gamma_b = -1$) strip elements with $l_a = l_b = 1.2\lambda_0$, and $d_a = 2.5\lambda_0$. (a) Periodic ($d_b = d_a$); (b) Fibonacci; (c) TM; (d) PD; (e) RS; (f) Bernoulli random [$\mathrm{prob}(a) = \mathrm{prob}(b) = 0.5$]. For all aperiodic arrays, $d_b = 1.6d_a$ is assumed. In (a)–(c), as a reference, the dominant BM peaks are labeled according to the asymptotic (infinite-array) predictions.

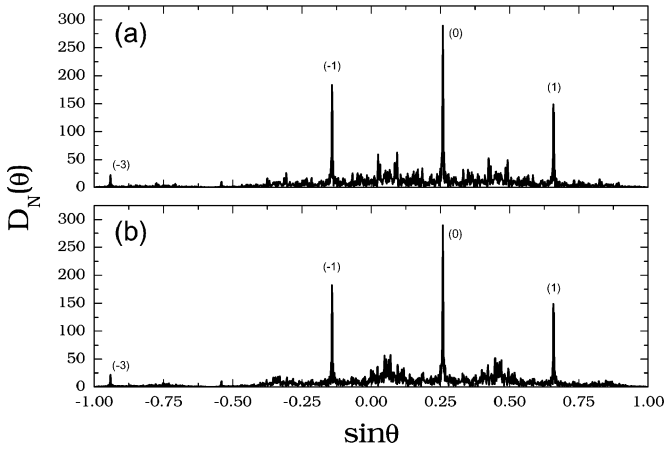

Fig. 3. As in Fig. 2, but with $d_b = 2d_a$. (a) RS and (b) Bernoulli random [$\mathrm{prob}(a) = \mathrm{prob}(b) = 0.5$]. As a reference, the dominant BM peaks are labeled according to the asymptotic (infinite-array) predictions in (8).

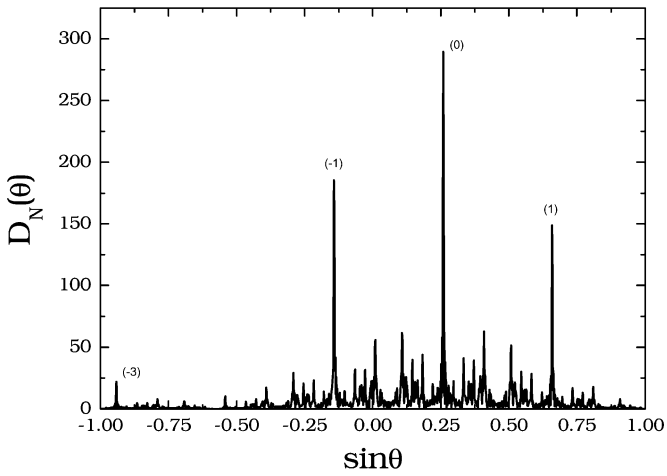

Fig. 4. As in Fig. 3, but for PD array.

and identical scale-ratio. The arrays are generated iterating the substitution rules in Sections III-B.2–III-B.5, namely, Fibonacci [Fig. 2(b)], TM [Fig. 2(c)], PD [Fig. 2(d)], and RS [Fig. 2(e)], using an "a" seed and taking the first 100 symbols. In these examples, in order to emphasize the possible *nontrivial* BM spectral features, an *effectively irrational* scale-ratio was chosen (recall the discussion in Section III-C); it was verified that a value $d_b/d_a = 5/4 = 1.6$ was sufficient to drive the higher-order trivial BM peaks outside the visible range $|k_x| \leq k_0$. Also displayed, as references examples, are the RCS responses of a *periodic* ($d_a = d_b$) array [Fig. 2(a)] and of a Bernoulli-type *random* array with $\mathrm{prob}(a) = \mathrm{prob}(b) = 0.5$ and $d_b = 1.6d_a$ [Fig. 2(f)]. Sharply localized peaks, with various structures and amplitudes [also modulated by the SESR in (2)], are clearly visible in all plots. More specifically, for the chosen parameter configuration, Fig. 2(b) is representative of the *quasiperiodic* BM spectrum in (12), whose complex structure (remarkably different from the periodic case) is clearly observable. As a reference, the labeling scheme in Fig. 2(b) associates some of the dominant peaks with the corresponding lowest-order (m, n)-indexed BM in (12). Conversely, the RCS response in Fig. 2(c) should be interpreted in terms of the superposition of a dominant *periodic-like* BM spectrum [cf. (14)] superposed onto a diffused singular-continuous spectrum [cf. (15), (16)]. Finally, the RCS responses in Fig. 2(d)–(f) turn out to exhibit only one strong peak (trivial specular-reflection BM) superposed onto background spectra with complicated structures [singular-continuous for the PD array in Fig. 2(d), and absolutely-continuous for the RS and random arrays in Fig. 2(e) and (f)]. Here and henceforth, the visual similarities between the responses of the *fully-deterministic* RS sequences and the Bernoulli-type *random* sequences are not coincidental. Indeed, it can be shown that the two sequences share *the same* spectral signatures [36].

To highlight the role of the scale-ratio, Fig. 3 displays the RCS responses of the same RS and random arrays in Fig. 2(e) and (f), but this time with an integer scale-ratio $d_b/d_a = 2$ which now renders the trivial BM spectrum in (8) clearly observable in the visible spectral range, superposed onto an absolutely-continuous spectral background. A similar trivial BM signature can be observed for the PD array in Fig. 4, but this time superposed onto a singular-continuous background. The same PD array, with a regular inter-element spacing $d_a = d_b$ but non-identical strips (e.g., $\Gamma_b \neq \Gamma_a$), exhibits a completely different RCS response, representative of the *infinite-periodic* BM spectrum in (20). An example is shown in Fig. 5, where at least three l-orders are observable.

B. Single-Element Scattering Response

As already observed, the BM wavenumbers depend on the substitution matrix and possibly on the scale-ratio. However, the modal excitation amplitudes also depend on the SESR in (2), which can be controlled by acting on the strip widths ($l_{a,b}$) and/or their constitutive properties (embedded in $\Gamma_{a,b}$). In this connection, analytic knowledge of the BM amplitudes can suggest particularly interesting parameter tunings, such the one in (10) which yields strong suppression of the trivial BM spectrum.

Within the calibrated parametric range of validity of our PO model, the strip width cannot be too small (in view of the Kirchhoff approximation) or too large (in view of the neglected inter-element coupling). In our simulations, values $l_{a,b} \geq 1.2\lambda_0$ are considered, always ensuring edge-to-edge inter-element distances $> \lambda_0/2$. Within this parametric ranges, changing the

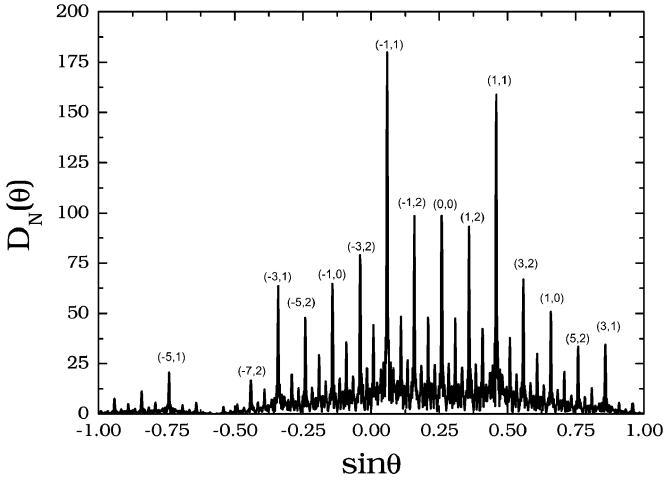

Fig. 5. As in Fig. 4 (PD array), but with $d_b = d_a$ and non-identical PEC $(\Gamma_a = -1)$ and PMC $(\Gamma_b = 1)$ strip elements. As a reference, some of the dominant trivial BM peaks are labeled according to the asymptotic (infinite-array) predictions in (20).

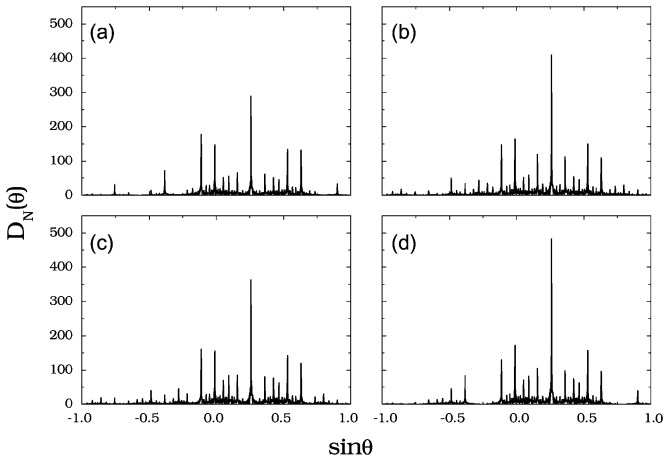

Fig. 6. As in Fig. 2(b) (Fibonacci array), but with $d_a = 3\lambda_0$ and various strip widths. (a) $l_a = l_b = 1.2\lambda_0$; (b) $l_a = 2\lambda_0, l_b = 1.2\lambda_0$; (c) $l_a = 1.2\lambda_0, l_b = 2\lambda_0$; (d) $l_a = l_b = 2\lambda_0$.

strip widths typically affects the RCS response in terms of a moderate re-shaping of the BM amplitudes, as shown in Fig. 6 for the Fibonacci case.

More suggestive may appear acting on the constitutive properties of the strips. Besides the rather trivial device of constructing *lacunary* arrays by setting to zero one of the reflection coefficients [see the example in Fig. 7 pertaining to RS and random arrays exhibiting trivial BM spectra similar to those in Fig. 3], such interest in motivated by the recent advances in the practical synthesis of artificial impedance surfaces (see, e.g., [43]) which are expected to provide new perspectives and additional degrees of freedom in the choice of $\Gamma_{a,b}$. As an illustrative example, Fig. 8(a) shows the RCS response of a TM array made of PEC $(\Gamma_a = -1)$ and ideal PMC $(\Gamma_b = 1)$ strips with equal inter-element spacing $d_a = d_b = 2.5\lambda_0$, which [recalling (10)] is characterized by a *purely singular-continuous* spectrum. A similar, purely singular-continuous, response can be obtained by properly tuning the parameters of a PD array, as shown in Fig. 8(b). These responses look very complicated,

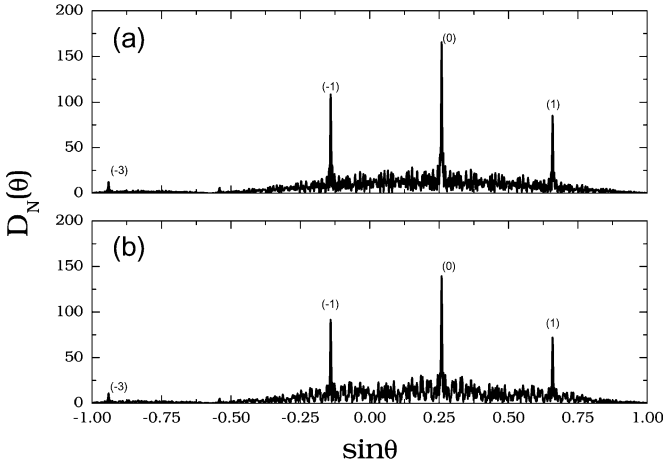

Fig. 7. As in Fig. 2, but with $d_a = d_b = 2.5\lambda_0$ and lacunary arrays $(\Gamma_a = -1, \Gamma_b = 0)$. (a) RS and (b) Bernoulli random $[\mathrm{prob}(a) = \mathrm{prob}(b) = 0.5]$.

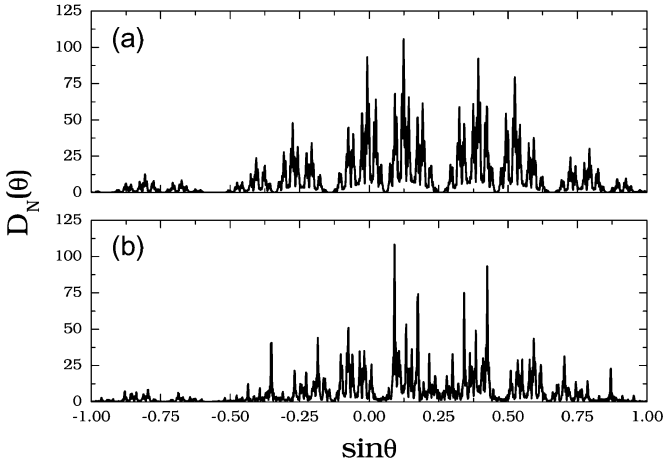

Fig. 8. As in Fig. 2, but with $d_a = d_b = 2.5\lambda_0$. (a) TM array with PEC $(\Gamma_a = -1)$ and PMC $(\Gamma_b = 1)$ strip elements; (b) PD array with $d_b = 1.6d_a, \Gamma_a = 0.5$, and $\Gamma_b = -1$.

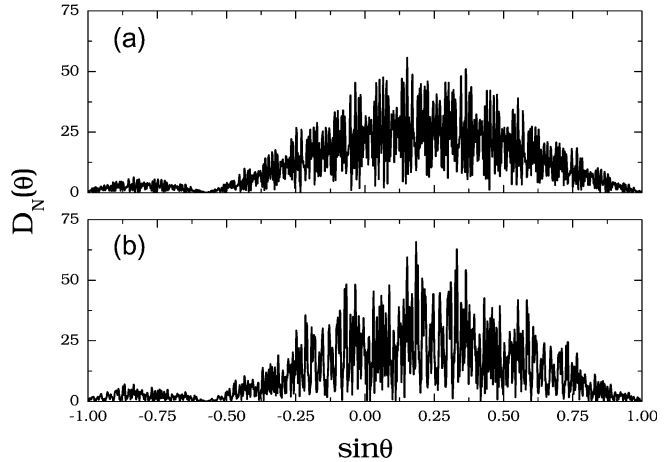

Fig. 9. As in Fig. 7, but with PEC $(\Gamma_a = -1)$ and PMC $(\Gamma_b = 1)$ strip elements.

and the limited spectral resolution available prevents full observation of the underlying scale richness (see the discussion in Section IV.C below). As a further example, Fig. 9 shows the

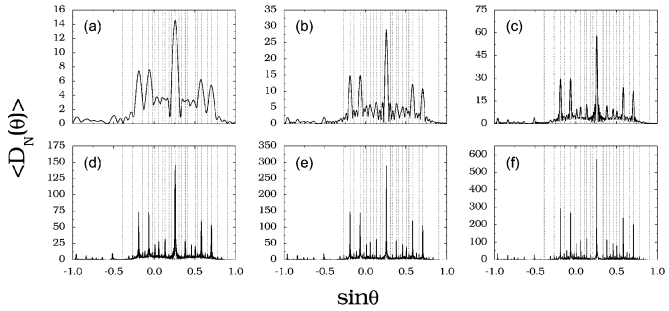

Fig. 10. Fibonacci array, as in Fig. 2(b). RCS response averaged over 1000 realizations (randomly chosen from a 10^5-element sequence). (a) $N = 5$; (b) $N = 10$; (c) $N = 20$; (d) $N = 50$; (e) $N = 100$; (f) $N = 200$. As a reference, the asymptotic (infinite-array) predictions in (12) for the quasiperiodic BM spectrum are displayed as dashed grids (for the sake of readability, only the orders $|m|, |n| \leq 4$ are shown).

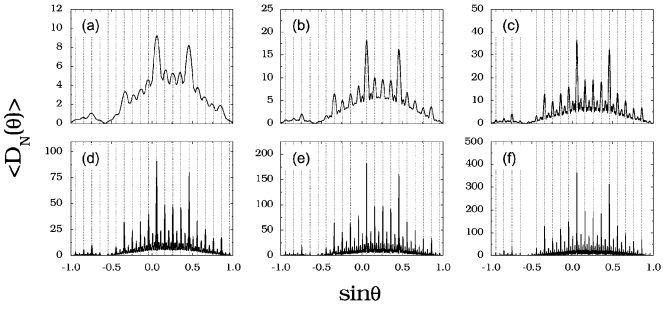

Fig. 11. As in Fig. 10, but for PD array with $d_a = d_b = 2.5\lambda_0$, and PEC ($\Gamma_a = -1$) and PMC ($\Gamma_b = 1$) strips. As a reference, the asymptotic (infinite-array) predictions in (18) for the infinite-periodic BM spectrum are displayed as dashed grids (for the sake of readability, only the orders $l \leq 2$ are shown).

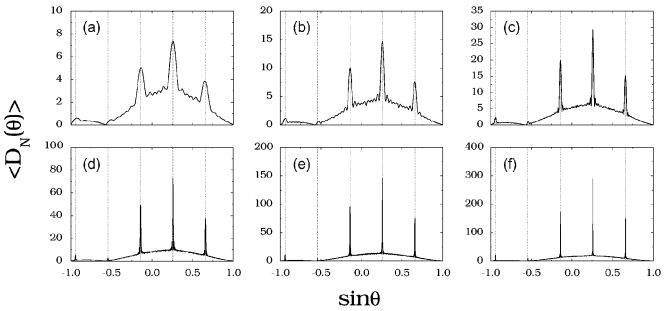

Fig. 12. As in Fig. 10, but for lacunary ($\Gamma_a = -1, \Gamma_b = 0$) RS array with $d_a = d_b = 2.5\lambda_0$. As a reference, the asymptotic (infinite-array) predictions in (8) for the trivial BM spectrum are displayed as dashed grids.

RCS responses of RS and random arrays made of evenly-spaced PEC/PMC strips, which [in view of (10)] exhibit purely absolutely-continuous spectra. Accordingly, these responses turn out to be devoid of any distinct localized footprints, and are essentially representative of the sinc-type SESR in (2).

C. Array Size

As illustrated in Section III, in the *infinite-array* limit, the scattering signatures of arrays based on substitutional sequences are essentially dictated by the substitution matrix in (5), and hence by the *global* symbol proportions rather than the actual *local* ordering. For *truncated*, relatively large-size arrays, like those in the numerical examples presented so far, one expects the above results to still be capable of predicting the positions of the dominant spectral peaks. However, in view of the limited ($\sim 1/N$) spectral resolution, and the typically *dense* character of certain BM spectra [see, e.g., (12) and (20)], such peaks (as well as the background structure) may actually be representative of *modal clusters*. Conversely, for relatively small-size arrays, one intuitively expects the *local* symbol ordering to play a more significant role.

In [21], we applied the results in Section III.B.2 to the study of large truncated Fibonacci-type arrays, via the use of generalized Poisson summation and via geometrical-diffraction-theory asymptotic parameterizations. Here, we address the study of the *global* versus *local* ordering effects via a statistical analysis of the RCS response in (24) for different array sizes. For a given substitution rule, the statistical population is constructed by generating a 10^5-element sequence (with "a" seed) and by randomly extracting 1000 different realizations of a given size. As a first example, Fig. 10 shows the average RCS response (denoted as $\langle D_N \rangle$) for a Fibonacci array of size $N = 5, 10, 20, 50, 100$, and 200. As a reference, the asymptotic (infinite-array) predictions in (12) for the purely quasiperiodic BM spectrum are displayed as dashed grids (for the sake of readability, only the orders $|m|, |n| \leq 4$ are shown). As expected, the spectral resolution increases with the array size, displaying a progressively finer structure in progressively closer agreement with the asymptotic predictions. Qualitatively similar behaviors are observed for the case of a PD array (see Fig. 11) characterized by an infinite-periodic BM spectrum and a singular-continuous background, and for a RS array (see Fig. 12) characterized by a trivial BM spectrum and an absolutely-continuous background.

We also studied the (normalized) standard deviation

$$\bar{\sigma}_N(\theta) = \frac{\sqrt{\langle D_N^2(\theta) \rangle - \langle D_N(\theta) \rangle^2}}{\max_\theta D_N(\theta)} \tag{25}$$

which quantifies the local-ordering-induced fluctuations in the RCS responses of different realizations. Intuitively, such effects are expected to be significant for relatively small-size arrays (where the local ordering plays a major role), and to become negligible for large-size arrays (where the response is dominated by the *global* symbol proportions). Fig. 13 shows the (maximum over θ) normalized standard deviation in (25), as a function of the array size N, for the examples in Figs. 10–12. As expected, the standard deviation decreases monotonically with the array size. For the Fibonacci case, one observes a decrease of one order of magnitude, from $\bar{\sigma}_5 = 0.15$ to $\bar{\sigma}_{200} = 0.012$. The slightly larger values observed for the other two examples (PD and RS) can be attributed to the presence of diffused spectral backgrounds.

The effects of the array-size in the diffused spectral constituents are less intuitive. The reader is referred to [22] for a study of the truncation effects in RS arrays (exhibiting absolutely-continuous spectral backgrounds) via numerical exploration of typical array-oriented observables such as directivity and sidelobe level. More complicated and *richer* in structure are the signatures associated with the singular-continuous background, typically characterized by *multifractal*

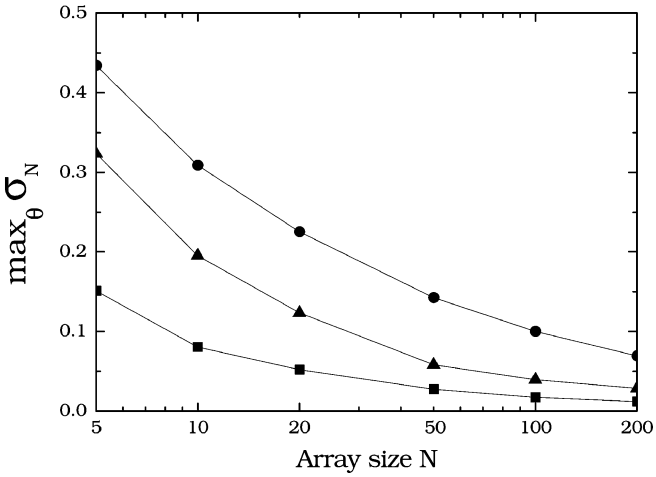

Fig. 13. As in Figs. 10–12, but (maximum over θ) normalized standard deviation in (25) as a function of array size N. Squares: Fibonacci (cf. Fig. 10); Triangles: PD (cf. Fig. 11); Circles: RS (cf. Fig. 12).

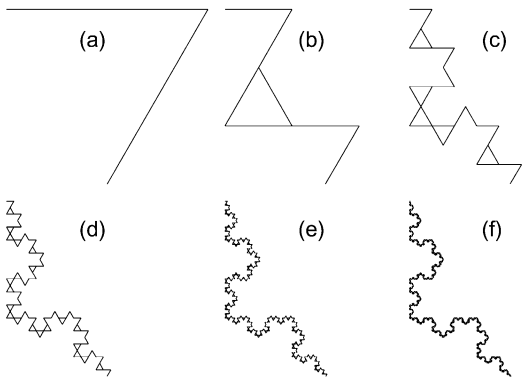

Fig. 14. Graphic illustration of the multifractal scaling properties of singular-continuous spectral constituents pertaining to a TM array configuration. Complex plots (real versus imaginary part) of the sequence of complex scattered fields associated with various structure sizes, $E_0^s = 0, E_1^s, \ldots, E_N^s$, for various values of N. Parameters as in Fig. 7(a), with reference to the modal wavenumber k_{x12} in (15), with scaling exponent $\alpha(k_{x12}) = \log 3/\log 2$. (a) $N = 2$; (b) $N = 8$; (c) $N = 32$; (d) $N = 128$; (e) $N = 512$; (f) $N = 2048$. As N increases, the resulting curves approach a *snowflake*-type fractal curve with dimension $D_F = \log 4/\log 3 \approx 1.262$.

scaling [25]–[27], [40], [41]. A simple way to graphically visualize such complex scaling properties is to plot, in the complex plane, the sequence of complex scattered fields associated with various structure sizes, $E_0^s = 0$, $E_1^s, \ldots, E_N^s$, successively, and to join E_n^s with E_{n+1}^s, $n = 0, 1, \ldots, N$. It can be shown that, for a spectral wavenumber $\bar{k}_x$ corresponding to a singular- continuous constituent with scaling exponent $\alpha(\bar{k}_x)$, the resulting plot tends (as $N \to \infty$) to a *fractal* curve with fractal dimension [25] $D_F = 2/\alpha(\bar{k}_x)$. As an illustration, Fig. 14 shows different iterations of such plots pertaining to the TM parameter configuration in Fig. 7(a), with reference to the modal wavenumber k_{x12} in (15), with scaling exponent $\alpha(k_{x12}) = \log 3/\log 2$. The resulting curves are observed to approach a typical *snowflake* fractal curve with dimension $D_F = \log 4/\log 3 \approx 1.262$. The reader is referred to [41], where *multiresolution* wavelet processing has been successfully applied, within the context of crystallography, to extract the scaling footprints pertaining to singular-continuous constituents in TM and PD geometries.

D. Remarks

The examples presented so far illustrate, an an introductory level, the wealth of scattering signatures exhibited by the seemingly-simple 1-D substitutional-sequence-based scenario considered, which spans the "gray-zone" from *quasiperiodic* to *quasirandom*. The distinctive characteristics of these signatures stem from the structure of the BM constituents and the diffused (singular-continuous and absolutely-continuous) background. It is worth pointing out that there are several examples of *completely different* geometries (e.g., periodic, TM, PD, RS) which, under appropriate parameter configurations, can give rise to *hardly distinguishable* BM signatures. In these cases, a key role is assumed by the (possible) *diffused background*, which can hide very complicated structures and surprising characteristics (see, e.g., [36]). From the above results, one is also led to the somehow counterintuitive considerations that, under appropriate conditions, *deterministic* geometries [e.g., the RS in Fig. 9(a)] can give rise to flat noise-like scattering signatures (typical of *random disorder*), whereas *random* geometries [e.g., the Bernoulli-type in Figs. 3(b) and 7(b)] can exhibit sharp BM signatures (typical of *periodic order*).

V. Conclusion

In this paper, we have addressed the study of plane-wave scattering from rather general 1-D aperiodically-ordered strip-array geometries based on two-symbol substitution rules. Within the framework of Kirchhoff PO approximation, it has been shown that, despite the rather general and complex character of the geometries involved, analytic parameterization and physical interpretation of the relevant aperiodic-order-induced wave phenomenologies can be addressed by exploiting theoretical results from solid-state physics and discrete geometry.

The results illustrated, via several representative examples, indicate that a wealth of scattering signatures, with (sometime counter-intuitive) spectral characteristics ranging from *quasiperiodic* to *quasirandom*, can be obtained via judicious exploitation of the additional geometrical and/or constitutive degrees of freedom available in aperiodic configurations. In particular, the role played by the substitution rule (and, specifically, the arithmetical properties of the associated substitution matrix), the scale-ratio, the SESR, and the array size, has been highlighted. From the application viewpoint, the richness of the radiation/scattering signatures of more *orderly* (e.g., quasiperiodic) configurations could be exploited for synthesis and control of peculiar EM responses of potential interest for radio-frequency identification. On the other hand, the more *random* looking responses (e.g., RS [22]) could be exploited for suppression of specular reflection (e.g., simulated rough surfaces [44] and "virtual shaping" [45]), of potential interest for radar countermeasures. Accordingly, we are planning current and future investigations of more *realistic* models, with the development of full-wave tools which account for the inter-element coupling as well as for the presence of well-characterized artificial surfaces (and thus angle- and frequency-dependent reflection coefficients). Also of interest, is a sensitivity analysis of the scattering signatures (e.g., with respect to scale-ratio,

strip-width, etc.) as well as the study of phenomena like enhanced backscattering or enhanced normal scattering, typical of disordered structures.

ACKNOWLEDGMENT

The authors also wish to thank an anonymous reviewer for useful comments and suggestions.

REFERENCES

[1] B. Grünbaum and G. C. Shepard, *Tilings and Patterns*. New York, NY: Freeman, 1987.

[2] M. Senechal, *Quasicrystals and Geometry*. Cambridge, U.K.: Cambridge Univ. Press, 1995.

[3] M. Baake, , J.-B. Suck, M. Schreiber, and P. Häussler, Eds., "A guide to mathematical quasicrystals," in *Quasicrystals: An Introduction to Structure, Physical Properties, and Applications*. Berlin, Germany: Springer, 2002, pp. 17–48.

[4] D. Shechtman, I. Blech, D. Gratias, and J. W. Cahn, "Metallic phase with long-range orientational order and no translation symmetry," *Phys. Rev. Lett.*, vol. 53, no. 20, pp. 1951–1953, Nov. 1984.

[5] D. Levine and P. J. Steinhardt, "Quasicrystals: A new class of ordered structures," *Phys. Rev. Lett.*, vol. 53, no. 26, pp. 2477–2480, Dec. 1984.

[6] D. Würtz, T. Schneider, and M. P. Soerensen, "Electromagnetic wave propagation in quasiperiodically stratified media," *Physica A*, vol. 148, no. 1–2, pp. 343–355, Feb. 1988.

[7] Y. S. Chan, C. T. Chan, and Z. Y. Liu, "Photonic band gaps in two dimensional photonic quasicrystals," *Phys. Rev. Lett.*, vol. 80, no. 5, pp. 956–959, Feb. 1998.

[8] M. S. Vasconcelos, E. L. Albuquerque, and A. M. Mariz, "Optical localization in quasi-periodic multilayers," *J. Phys.: Condens. Matter*, vol. 10, no. 26, pp. 5839–5849, July 1998.

[9] E. Maciá, "Optical engineering with Fibonacci dielectric multilayers," *Appl. Phys. Lett.*, vol. 73, no. 23, pp. 3330–3332, Dec. 1998.

[10] C. Jin, B. Cheng, B. Man, Z. Li, D. Zhang, S. Ban, and D. Sun, "Band gap and wave guiding effect in a quasiperiodic photonic crystal," *Appl. Phys. Lett.*, vol. 75, no. 13, pp. 1848–1850, Sept. 1999.

[11] C. Jin, B. Cheng, B. Man, Z. Li, and D. Zhang, "Two-dimensional dodecagonal and decagonal quasiperiodic photonic crystals in the microwave region," *Phys. Rev. B*, vol. 61, no. 16, pp. 10762–10767, Apr. 2000.

[12] M. A. Kaliteevski, S. Brand, R. A. Abram, T. F. Krauss, R. M. De La Rue, and P. Millar, "Two-dimensional Penrose-tiled photonic quasicrystals: Diffraction of light and fractal density of modes," *J. Mod. Opt.*, vol. 47, no. 11, pp. 1771–1778, Nov. 2000.

[13] X. Zhang, Z.-Q. Zhang, and C. T. Chan, "Absolute photonic band gaps in 12-fold symmetric photonic quasicrystals," *Phys. Rev. B*, vol. 63, no. 8, Feb. 2001, 081105(R).

[14] M. Bayndir, E. Cubukcu, I. Bulu, and E. Ozbay, "Photonic band-gap effect, localization, and waveguiding in the two-dimensional Penrose lattice," *Phys. Rev. B*, vol. 63, no. 16, Apr. 2001, 161104(R).

[15] M. Hase, H. Miyazaki, M. Egashira, N. Shinya, K. M. Kojima, and S. Uchida, "Isotropic photonic band gap and anisotropic structures in transmission spectra of two-dimensional fivefold and eightfold symmetric quasiperiodic photonic crystals," *Phys. Rev. B*, vol. 66, no. 21, Dec. 2002, 214205.

[16] Z. Ouyang, C. Jin, D. Zhang, B. Cheng, X. Meng, G. Yang, and J. Li, "Photonic bandgaps in two-dimensional short-range periodic structures," *J. Opt. A: Pure Appl. Opt.*, vol. 4, no. 1, pp. 23–28, Jan. 2002.

[17] A. Della Villa, S. Enoch, G. Tayeb, V. Pierro, V. Galdi, and F. Capolino, "Bandgap formation and multiple scattering in photonic quasicrystals with a Penrose-type lattice," *Phys. Rev. Lett.*, vol. 94, no. 18, May 2005, 183903.

[18] A. Della Villa, V. Galdi, F. Capolino, V. Pierro, S. Enoch, and G. Tayeb, "A comparative study of representative categories of EBG dielectric quasicrystals," *IEEE Antennas Wireless Propag. Lett.*, vol. 5, pp. 331–334, 2006.

[19] A. Della Villa, S. Enoch, G. Tayeb, F. Capolino, V. Pierro, and V. Galdi, "Localized modes in photonic quasicrystals with Penrose-type lattice," *Optics Express*, vol. 14, no. 21, pp. 10021–10027, Oct. 2006.

[20] V. Pierro, V. Galdi, G. Castaldi, I. M. Pinto, and L. B. Felsen, "Radiation properties of planar antenna arrays based on certain categories of aperiodic tilings," *IEEE Trans. Antennas Propag.*, vol. 53, no. 2, pp. 635–644, Feb. 2005.

[21] V. Galdi, G. Castaldi, V. Pierro, I. M. Pinto, and L. B. Felsen, "Parameterizing quasiperiodicity: Generalized Poisson summation and its application to modified-Fibonacci antenna arrays," *IEEE Trans. Antennas Propag.*, vol. 53, no. 6, pp. 2044–2053, June 2005.

[22] V. Galdi, V. Pierro, G. Castaldi, I. M. Pinto, and L. B. Felsen, "Radiation properties of one-dimensional random-like antenna arrays based on Rudin-Shapiro sequences," *IEEE Trans. Antennas Propag.*, vol. 53, no. 11, pp. 3568–3575, Nov. 2005.

[23] E. Bombieri and J. E. Taylor, "Which distributions of matter diffract? An initial investigation," *J. Physique France*, vol. 47, pp. 19–28, 1986, Colloque C3.

[24] E. Bombieri and J. E. Taylor, "Quasicrystals, tilings, and algebraic number theory: Some preliminary connections," *Contemporary Mathematics*, vol. 64, pp. 241–264, 1987.

[25] S. Aubry, C. Godrèche, and J. M. Luck, "Scaling properties of a structure intermediate between quasiperiodic and random," *J. Stat. Phys.*, vol. 51, no. 5/6, pp. 1033–1075, June 1988.

[26] J. M. Luck, "Cantor spectra and scaling of gap widths in deterministic aperiodic systems," *Phys. Rev. B*, vol. 39, no. 9, pp. 5834–5849, Mar. 1989.

[27] C. Godrèche and J. M. Luck, "Multifractal analysis in reciprocal space and the nature of the fourier transform of self-similar structures," *J. Phys. A: Math. Gen.*, vol. 23, no. 16, pp. 3769–3797, Aug. 1990.

[28] M. Kolář, "New class of one-dimensional quasicrystals," *Phys. Rev. B*, vol. 47, no. 9, pp. 5489–5492, Mar. 1993.

[29] M. Kolář, B. Iochum, and L. Raymond, "Structure factor of 1D systems (superlattices) based on two-letter substitution rules: I. δ (Bragg) peaks," *J. Phys. A: Math. Gen.*, vol. 26, no. 24, pp. 7343–7366, Dec. 1993.

[30] L. Carin and L. B. Felsen, "Time-harmonic and transient scattering by finite periodic flat strip arrays: Hybrid (Ray)-(Floquet mode)-(MOM) algorithm and its GTD interpretation," *IEEE Trans. Antennas Propag.*, vol. 41, no. 4, pp. 412–421, Apr. 1993.

[31] L. B. Felsen and L. Carin, "Diffraction theory of frequency- and time-domain scattering by weakly aperiodic truncated thin-wire gratings," *J. Opt. Soc. Amer. A*, vol. 11, no. 4, pp. 1291–1306, Apr. 1994.

[32] L. Carin and L. B. Felsen, "Wave-oriented data processing for frequency- and time-domain scattering by nonuniform arrays," *IEEE Antennas Propag. Mag.*, vol. 36, no. 3, pp. 29–43, Jun. 1994.

[33] M. McClure, D. Kralj, T.-T. Hsu, L. Carin, and L. B. Felsen, "Frequency-domain scattering by nonuniform truncated arrays: Wave-oriented data processing for inversion and imaging," *J. Opt. Soc. Amer. A*, vol. 11, no. 10, pp. 2675–2684, Oct. 1994.

[34] L. B. Felsen and E. Gago-Ribas, "Ray theory for scattering by two-dimensional quasiperiodic plane finite arrays," *IEEE Trans. Antennas Propag.*, vol. 44, no. 3, pp. 375–382, Mar. 1996.

[35] J. Baldauf, S. W. Lee, H. Ling, and R. Chou, "On physical optics for calculating scattering from coated bodies," *J. Electromagn. Waves Appl.*, vol. 3, no. 8, pp. 725–746, Aug. 1989.

[36] M. Höffe and M. Baake, "Surprises in diffuse scattering," *Zeitschrift für Kristallographie*, vol. 215, no. 8, pp. 441–444, Aug. 2000.

[37] M. Queffélec, "Substitution Dynamical Systems—Spectral Analysis," in *Lecture Notes in Mathematics*. Berlin: Springer, 1987, vol. 1294.

[38] N. P. Fogg, V. Berthé, S. Ferenczi, C. Mauduit, and A. Siegel, Eds., "Substitutions in Dynamics, Arithmetics, and Combinatorics," in *Lecture Notes in Mathematics*. Berlin: Springer, 2002, vol. 1794.

[39] Z. Cheng, R. Savit, and R. Merlin, "Structure and electronic properties of Thue-Morse lattices," *Phys. Rev. B*, vol. 37, no. 9, pp. 4375–4382, Mar. 1988.

[40] Z. Cheng and R. Savit, "Multifractal properties of the structure factor of a class of substitutional sequences," *Phys. Rev. A*, vol. 44, no. 10, pp. 6379–6385, Nov. 1991.

[41] E. Liviotti, "A study of the structure factor of Thue-Morse and period-doubling chains by wavelet analysis," *J. Phys.: Condens. Matter*, vol. 8, no. 27, pp. 5007–5015, July 1996.

[42] Z. Masáková, J. Patera, and E. Pelantová, "Minimal distances in quasicrystals," *J. Phys. A: Math. Gen.*, vol. 31, no. 6, pp. 1539–1552, Feb. 1998.

[43] P.-S. Kildal, A. Kishk, and S. Maci, Guest Editors, *IEEE Trans. Antennas Propag., Special Issue on "Artificial Magnetic Conductors, Soft/Hard Surfaces, and other Complex Surfaces"*, vol. 53, no. 1, Jan. 2005.

[44] D. S. Stephen, T. Mathew, K. A. Jose, C. K. Aanandan, P. Mohanan, and K. G. Nair, "New simulated corrugated scattering surface giving wideband characteristics," *Electron. Lett.*, vol. 29, no. 4, pp. 329–331, Feb. 1993.

[45] J. R. Swandic, "Bandwidth limits and other considerations for monostatic RCS reduction by virtual shaping," Naval Surface Warfare Center, Carderock Div., Bethesda, MD, Tech. Rep. A927224, Jan. 2004.

Vincenzo Galdi (M'98–SM'04) was born in Salerno, Italy, on July 28, 1970. He received the Laurea degree (*summa cum laude*) in electrical engineering and the Ph.D. degree in applied electromagnetics from the University of Salerno, Italy, in 1995 and 1999, respectively.

From April to December 1997, he held a visiting position in the Radio Frequency Division of the European Space Research & Technology Centre (ESTEC-ESA), Noordwijk, The Netherlands. From September 1999 to August 2002, he held a postdoctoral research associate position in the Department of Electrical and Computer Engineering at Boston University, Boston, MA. In November 2002, he was appointed Associate Professor of Electromagnetics, and joined the Department of Engineering at the University of Sannio, Benevento, Italy, where, since February 2005, he has been serving as Associate Chair for Undergraduate Studies in Telecommunication Engineering. From July to August 2006, within the framework of the Laser Interferometer Gravitational-wave Observatory (LIGO) experiment, he held a visiting position at the Massachusetts Institute of Technology, Cambridge, MA, and at the California Institute of Technology, Pasadena, CA. He is the author or coauthor of over 100 papers published in peer-reviewed international journals and conference proceedings. His research interests include analytical and numerical techniques for wave propagation in complex environments, metamaterials, electromagnetic chaos, inverse scattering, and gravitational interferometry.

Dr. Galdi is the recipient of a 2001 International Union of Radio Science (URSI) "Young Scientist Award." He is a member of Sigma Xi, of the LIGO Scientific Collaboration (LSC), of the Italian Electromagnetic Society (SIEM), and of the Italian National Institute of Nuclear Physics (INFN).

Giuseppe Castaldi was born in Benevento, Italy, in 1968. He received the Laurea degree (*summa cum laude*) in electrical engineering from the "Federico II" University of Naples, Italy, in 1995, and the Ph.D. degree in applied electromagnetics from the University of Salerno, Italy, in 1999.

In 2001, he was a Postdoctoral Research Fellow at the TNO Physics and Electronics Laboratory, The Hague, The Netherlands. In 2003, he was appointed Assistant Professor of Electromagnetics and joined the Department of Engineering at the University of Sannio, Benevento, Italy, where he is currently working. His research interests include electromagnetic chaos, quasi-periodic antenna arrays, applications of neural networks to inverse scattering problems, and field representations in complex environments.

Vincenzo Pierro was born in Salerno, Italy, in 1967. He received the Laurea degree (*summa cum laude*) in physics from the University of Salerno, Italy, in 1990.

In 1991, he held a visiting position in the COLUMBUS Metrology Group at the European Space Research & Technology Centre (ESTEC-ESA), Noordwijk, The Netherlands. Since 1996, he has been with the Faculty of Engineering, University of Sannio, Benevento, Italy, where he was appointed Assistant Professor of Electromagnetics in 1996, and Associate Professor in 2001. In 1999, he was awarded a research fellowship from the Japan Society for the Promotion of Science (JSPS), in connection with the TAMA 300 experiment. His main research interests are in the field of complex electromagnetic systems, electromagnetic detection of gravitational waves, and applied mathematics.

Prof. Pierro is a member of the LIGO Scientific Collaboration (LSC), of the Italian National Institute of Nuclear Physics (INFN), and of the Italian Physical Society (SIF).

Innocenzo M. Pinto (M'99–SM'06) was born and educated in Italy. Winner of national competitions, he was appointed Assistant Professor of Electromagnetics in 1983, Aassociate Professor in 1987, and Full Professor in 1990. He has been faculty member in the Universities of Naples, Salerno (where he founded and chaired the Ph.D. program in Information Engineering from 1993–2001), Catania, and Sannio at Benevento, where he is currently working. He has visited several research institutions as an invited lecturer, including CERN, KEK, and NIST (former NBS). In 1998, he was an EU Senior Visiting Scientist at the National Astronomical Observatory, Tokyo, Japan, in connection with the TAMA300 experiment. He authored or coauthored more than 100 technical papers in peer-reviewed international journals. His research interest span from electrophysics to gravitational wave experiments.

Prof. Pinto is a member of the American Physical Society, of the LIGO Scientific Collaboration (LSC), of the Italian National Institute of Nuclear Physics (INFN), and of the Italian Electromagnetic Society (SIEM).

Leopold B. Felsen *deceased*, (S'47–M'54–SM'55–F'62–LF'90) was born in Munich, Germany, on May 7, 1924. He received the B.E.E., M.E.E, and D.E.E. degrees from the Polytechnic Institute of Brooklyn, Brooklyn, NY, in 1948, 1950, and 1952, respectively.

He emigrated to the United States in 1939 and served in the U.S. Army from 1943 to 1946. After 1952, he remained with the Polytechnic (now Polytechnic University), becoming University Professor in 1978. From 1974 to 1978, he was Dean of Engineering. In 1994, he resigned from the full-time Polytechnic faculty and was granted the status of University Professor Emeritus. He was Professor of aerospace and mechanical engineering and Professor of electrical and computer engineering at Boston University, Boston, MA (part-time). He was the author or coauthor of more than 350 papers and of several books, including *Radiation and Scattering of Waves* (Piscataway, NJ: IEEE Press, 1994). He was an Associate Editor of several professional journals and was an Editor of the *Wave Phenomena Series* (New York: Springer-Verlag). His research interests encompassed wave propagation and diffraction in complex environments and in various disciplines, high-frequency asymptotic and short-pulse techniques, and phase-space methods with an emphasis on wave-oriented data processing and imaging.

Dr. Felsen was a Member of Sigma Xi and a Fellow of the Optical Society of America and the Acoustical Society of America. He has held named Visiting Professorships and Fellowships at universities in the United States and abroad, including the Guggenheim in 1973 and the Humboldt Foundation Senior Scientist Award in 1981. In 1974 he was an IEEE Antennas and Propagation Society (APS) Distinguished Lecturer. His "Poet's Corner" appeared sporadically in the IEEE/APS Magazine. He received the IEEE/APS Best Paper Award for 1969 and was best paper coauthor for 1974 and 1981. He was a contributing author to papers selected for the R. W. P. King Award for 1984, 1986, and 2000. He received the Balthasar van der Pol Gold Medal from the International Union of Radio Science (URSI) in 1975, an Honorary Doctorate from the Technical University of Denmark in 1979, the IEEE Heinrich Hertz Gold Medal for 1991, the APS Distinguished Achievement Award for 1998, the IEEE Third Millennium Medal in 2000, an Honorary Laurea degree from the University of Sannio in Benevento, Italy in 2003, the IEEE Electromagnetics Award for 2003, an honorary doctorate from the Technical University of Munich, Germany in 2004, an Honorary Doctorate from Dogus University in Istanbul, Turkey, three Distinguished Faculty Alumnus Awards from Polytechnic University, and an IEEE Centennial Medal in 1984. In 1977, he was elected to the National Academy of Engineering. He served on the APS Administrative Committee from 1963 to 1966 and was Vice Chairman and Chairman for both the US (1966–1973) and the International (1978–1984) URSI Commission B.